Available online at www.sciencedirect.com

ScienceDirect

Publishing Services by Elsevier

International Journal of Naval Architecture and Ocean Engineering 10 (2018) 318–328
http://www.journals.elsevier.com/international-journal-of-naval-architecture-and-ocean-engineering/

Dynamic modeling and three-dimensional motion simulation of a disk type underwater glider

Pengyao Yu, Tianlin Wang*, Han Zhou, Cong Shen

Transportation Equipment and Ocean Engineering College, Dalian Maritime University, 116026 Dalian, Liaoning, China

Received 17 March 2017; revised 12 July 2017; accepted 1 August 2017
Available online 22 September 2017

Abstract

Disk type underwater gliders are a new type of underwater gliders and they could glide in various directions by adjusting the internal structures, making a turnaround like conventional gliders unnecessary. This characteristic of disk type underwater gliders makes them have great potential application in virtual mooring. Considering dynamic models of conventional underwater gliders could not adequately satisfy the motion characteristic of disk type underwater gliders, a nonlinear dynamic model for the motion simulation of disk type underwater glider is developed in this paper. In the model, the effect of internal masses movement is taken into consideration and a viscous hydrodynamic calculation method satisfying the motion characteristic of disk type underwater gliders is proposed. Through simulating typical motions of a disk type underwater glider, the feasibility of the dynamic model is validated and the disk type underwater glider shows good maneuverability.

Keywords: Underwater glider; Dynamic modeling; Viscous hydrodynamic modeling; Motion simulation

1. Introduction

Underwater gliders are a type of autonomous underwater vehicle that are driven by changing their buoyancy and position of mass center. They are characterized by low energy consumption, low cost and long range. Nowadays, several commercial gliders have been broadly applied in physical and biological oceanography, such as the *Slocum* (Webb et al., 2001), the *Spray* (Sherman et al., 2001) and the *Seaglider* (Eriksen et al., 2001).

Considering the role played by underwater gliders in ocean observation, much theoretical and experimental work has been carried out to promote the progress of underwater glider design technology. In Graver (2005) and Wang and Wang (2009), dynamic models of underwater gliders were established and the motion of gliders were simulated. In Leonard and Graver (2001), Bhatta and Leonard (2008) and Fan and Woolsey (2013), the nonlinear gliding stability and how to design stabilizing control laws for gliders were discussed. Mahmoudian et al. (2010) applied the perturbation theory to derive an approximate analytical solution for steady spiraling motion. The steady spiraling motion was also analyzed by Zhang et al. (2011, 2013) and a fast solution method for the steady spiraling motion was produced. To improve the maneuverability of gliders, the idea that placing propellers at the stern of original gliders has attracted many researches (Wang et al., 2011; Isa et al., 2014; Chen et al., 2016).

Breaking the shape of traditional underwater gliders, underwater gliders have entered into a diversified development stage. Zhang et al. (2012, 2014) designed a gliding robotic fish combining gliding and fin-actuation mechanisms. This Gliding robotic fish is essentially a hybrid of underwater gliders and robotic fish which is energy efficient and highly maneuverable. And it has been applied in the autonomous sampling of water columns in the Wintergreen Lake, Michigan (Zhang et al., 2016). Referring to air vehicles of circular plan-form,

* Corresponding author.
E-mail address: wangtianlin@dlmu.edu.cn (T. Wang).
Peer review under responsibility of Society of Naval Architects of Korea.

http://dx.doi.org/10.1016/j.ijnaoe.2017.08.002

Niewiadomska et al. (2003) designed a mobile and bottom-resting autonomous underwater glider, whose body was lenticular shape and a tail rudder was fixed at the end of the body. Nakamura et al. (2007) developed a disk type glider for virtual mooring. The concept of virtual mooring refers to the monitoring of local waters by underwater vehicles, as if underwater vehicles were mooring in local waters. When the vehicle deviates from the target position under the external disturbance, it should move back to the designated waters. The shape of the disk type glider (Nakamura et al., 2007) is axisymmetric and it does not have any appendage, such as propellers and rudders. By adjusting the mass center of the glider, it could glide in any directions around the disk. Nakamura et al. (2008) further designed the full-scale disk type glider "BOOMERANG" and the operational tests in the field were carried out. It can be seen that when the glider needs to change the direction of movement, the traditional underwater glider would have to turn the body, while the disk type glider only need to move the internal structure to change the mass center of the glider system, which means the disk type glider is more suitable for virtual mooring tasks.

The disk type underwater glider is a new type of underwater gliders and it has better maneuverability than conventional underwater gliders, which makes it potential in marine exploration. A reasonable dynamic model for the disk type underwater glider would be helpful to the prototype development and the design of control system. However, existed dynamic models of conventional underwater gliders often have such limitation that the drift angle cannot be too large, which means they could not satisfy the motion characteristic of disk type underwater gliders. Although the dynamic model of the disk type underwater glider has been discussed by Nakamura et al. (2007), the analytic method is still inadequate, such as effects of internal masses movement is ignored and calculation method of hydrodynamic force do not satisfy the omni-maneuverability of the disk type underwater glider. Therefore, the modeling and simulation of the disk type underwater glider is still a challenge.

Taking a disk type underwater glider as an example, a nonlinear dynamic model is derived in this paper. In the model, the glider was treated as a multi-particle system and the effect of internal masses movement is taken into consideration. Making use of the axisymmetric characteristic of the shape of the disk type underwater glider, a special viscous hydrodynamic calculation method is introduced which satisfies the omni-directional maneuverability of the disk type underwater glider. Based on the dynamic model, typical motions of the disk type underwater glider (sawtooth motion in horizontal direction, sawtooth motion in vertical direction and omni-directional motion) are simulated.

2. Dynamic model

The appearance of a disk type underwater glider is shown in Fig. 1 and internal structures of the glider are shown in Fig. 2. It can be seen that the disk type glider is composed of a rigid body (mass m_{rb}), two moving blocks (mass m_{p1} and m_{p2}),

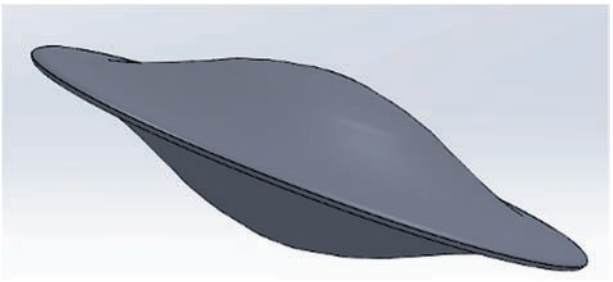

Fig. 1. Appearance of a disk type underwater glider.

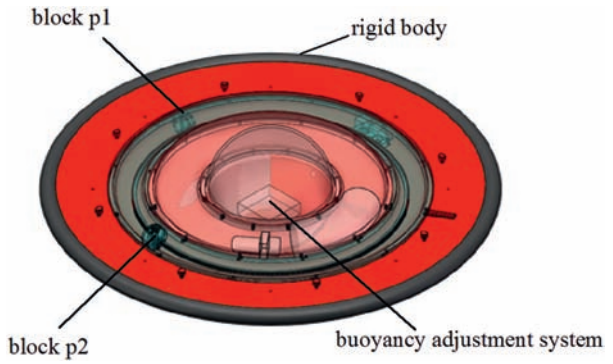

Fig. 2. Internal structures of the glider.

and a variable ballast actuator (mass m_{b}) for buoyancy adjustment. The moving blocks can move along the circle located in the symmetry plane of the upper and lower parts of the glider and they are represented as moving mass particles. The buoyancy adjustment system is represented as a variable mass m_{b} with fixed-position. During the analysis, the volume of the glider V_{dis} is regarded to be constant. Influenced by variable mass m_{b}, the total vehicle mass is variable, which can be expressed in the following equation

$$m = m_{rb} + m_{p1} + m_{p2} + m_b \tag{1}$$

The net weight of the glider can be described as

$$W = mg - \rho g V_{dis} \tag{2}$$

The change rate of the glider mass $\dot{m}_b$ is an input, affected by the buoyancy-powered propulsion. When W is greater than zero, the glider would tend to sink and when W is less than zero, the glider would tend to rise. Through moving blocks p1 and p2, the position of mass center would change, thus the adjustment of motion direction and attitude of the glider is realized. As shown in Fig. 3, Bc and Gc are respectively buoyancy center and mass center of the glider and two different attitudes are described by different colors. The rotation accelerations of two blocks $\ddot{\delta}_{p1}$ and $\ddot{\delta}_{p2}$ are the control inputs, which are used to adjust the positions of blocks.

2.1. Kinematics

Two coordinate frames are used to describe the motion of the disk type underwater glider. One is inertial coordinate frame and the other is body-fixed frame. As shown in Fig. 4, the inertial

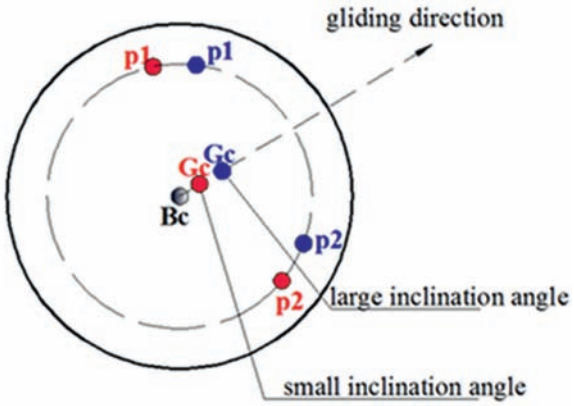

Fig. 3. Schematic diagram of blocks adjustment.

coordinate $E-\xi\eta\zeta$ is fixed at the inertial space and coordinate axis $E-\zeta$ is aligned with the force due to gravity. The origin of body frame $o-xyz$ is located at the buoyancy center of the glider. Coordinate plane $o-xy$ coincides with the symmetry plane between the upper and lower parts of the glider.

According to the classical robotics' knowledge, the kinematics for the glider can be written as

$$\dot{b} = R_{EB}v,\ \dot{R}_{EB} = R_{EB}\widehat{\omega} \tag{3}$$

where **b** is a vector from the origin of the inertial frame to buoyancy center of the glider, which is used to express the position of underwater glider in the inertial frame. R_{EB} is a rotational transformed matrix from the body frame to the inertial frame. v and ω are respectively the linear and angular velocities of glider expressed in the body frame. The operator '$\widehat{\cdot}$' maps a vector to a 3×3 skew-symmetric matrix, which satisfies $\widehat{a}c = a\times c$ for vectors a and c.

Generally, the attitude of underwater gliders in inertial coordinate frame can be described with Euler angle $\boldsymbol{\Omega}$ (roll angle φ, pitch angle θ and yaw angle ψ) and the relationship between the Euler angles rates and the angular velocity of the glider with respect to the body frame can be expressed in the following equation

$$\dot{\Omega} = R_{\Omega B}\omega \tag{4}$$

In order to facilitate the subsequent analysis, the coordinate of position and attitude of the glider in the inertial system and the linear and angular velocity of the glider with respect to the body frame are denoted as

$$b = \begin{bmatrix}\xi_B\\ \eta_B\\ \zeta_B\end{bmatrix},\ \Omega = \begin{bmatrix}\varphi\\ \theta\\ \psi\end{bmatrix},\ v = \begin{bmatrix}u\\ v\\ w\end{bmatrix},\ \omega = \begin{bmatrix}p\\ q\\ r\end{bmatrix} \tag{5}$$

Through the coordinate transformation, the transform matrixes R_{EB} and $R_{\Omega B}$ can be obtained which are determined by Euler angle Ω. And transform matrixes have the property like $R_{EB}^{-1} = R_{EB}^{T}$, $R_{\Omega B}^{-1} = R_{\Omega B}^{T}$. Using the simplified notation $c = \cos(\cdot)$, $s = \sin(\cdot)$ and $t = \tan(\cdot)$, R_{EB} and $R_{B\Omega}$, respectively have the form of

$$R_{EB} = \begin{bmatrix} c\theta c\psi & s\varphi s\theta c\psi - c\varphi s\psi & c\varphi s\theta c\psi + s\varphi s\psi \\ c\theta s\psi & c\varphi c\psi + s\varphi s\theta s\psi & -s\varphi c\psi + c\varphi s\theta s\psi \\ -s\theta & s\varphi c\theta & c\varphi c\theta \end{bmatrix},\ R_{B\Omega}$$
$$= \begin{bmatrix} 1 & 0 & -s\theta \\ 0 & c\varphi & s\varphi c\theta \\ 0 & -s\varphi & c\varphi c\theta \end{bmatrix} \tag{6}$$

In addition to the six degrees of freedom associated with the glider's translation and rotation, two blocks also can move in the body of the glider. The kinematics of the moving mass particles with respect to the inertial space is

$$v_{pi} = v + \omega \times r_{pi} + \dot{r}_{pi} \quad (i = 1,2) \tag{7}$$

where $v_{pi}(i=1,2)$ are the linear velocity of two moving mass particles with respect to the inertial frame, $r_{pi}(i=1,2)$ are the position of particles with respect to the body frame.

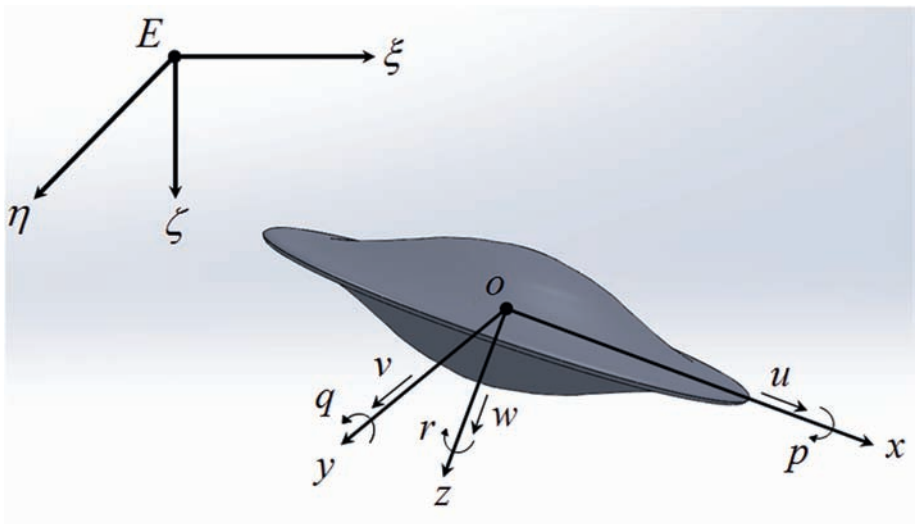

Fig. 4. Coordinate frames.

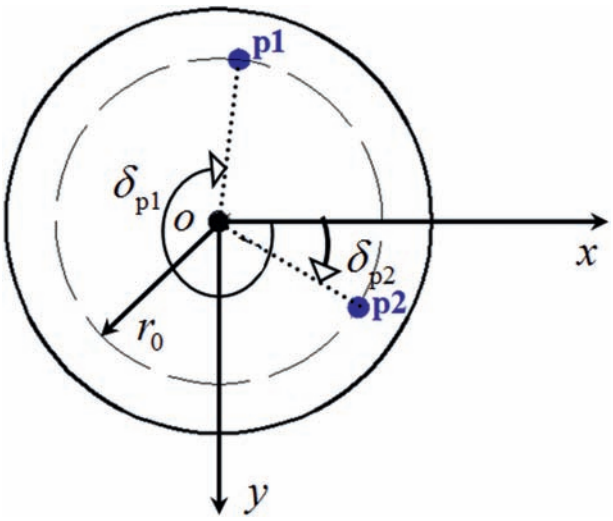

Fig. 5. Position description of two moving blocks.

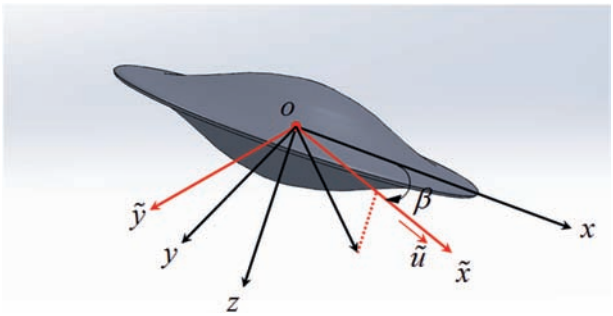

Fig. 6. Description of the direction coordinate frame.

In the $o-xy$ plane as shown in Fig. 5, the radius of motion trajectory of particles is r_0 and the center of the circle is located at the origin of body frame $o-xyz$. Considering rotation accelerations of two blocks $\ddot{\delta}_{pi}(i=1,2)$ are inputs, $r_{pi}, \dot{r}_{pi}, \ddot{r}_{pi}\ (i=1,2)$ should be expressed with $\delta_{pi},\ \dot{\delta}_{pi},\ \ddot{\delta}_{pi}(i=1,2)$.

$$r_{pi}=\begin{bmatrix} r_0 cos\delta_{pi} \\ r_0 sin\delta_{pi} \\ 0 \end{bmatrix},\ \dot{r}_{pi}=\begin{bmatrix} -r_0\dot{\delta}_{pi} sin\delta_{pi} \\ r_0\dot{\delta}_{pi} cos\delta_{pi} \\ 0 \end{bmatrix},\ \ddot{r}_{pi}$$
$$=\begin{bmatrix} -r_0\ddot{\delta}_{pi} sin\delta_{pi} - r_0\dot{\delta}_{pi}^2 cos\delta_{pi} \\ r_0\ddot{\delta}_{pi} cos\delta_{pi} - r_0\dot{\delta}_{pi}^2 sin\delta_{pi} \\ 0 \end{bmatrix}\quad (i=1,2) \tag{8}$$

where $\dot{\delta}_{pi}(i=1,2)$ are rotation velocities of the two blocks, $\ddot{\delta}_{pi}(i=1,2)$ are rotation accelerations of the two blocks.

2.2. Dynamics

The dynamics analysis is aimed at establishing the relationship between the motion and forces on the glider in the body coordinate frame. According to the momentum theorem, we know that

$$\dot{p}=G+B+f_v,\ \dot{\pi}=b_G\times G+b\times B+\tau_v \tag{9}$$

where $\mathbf{p}$ and $\boldsymbol{\pi}$ are respectively defined as the translational and angular momentum of the glider in the inertial frame. G is the gravity of the glider. B is the buoyancy of the glider. b_G and b are respectively position vectors of centers of the gravity and

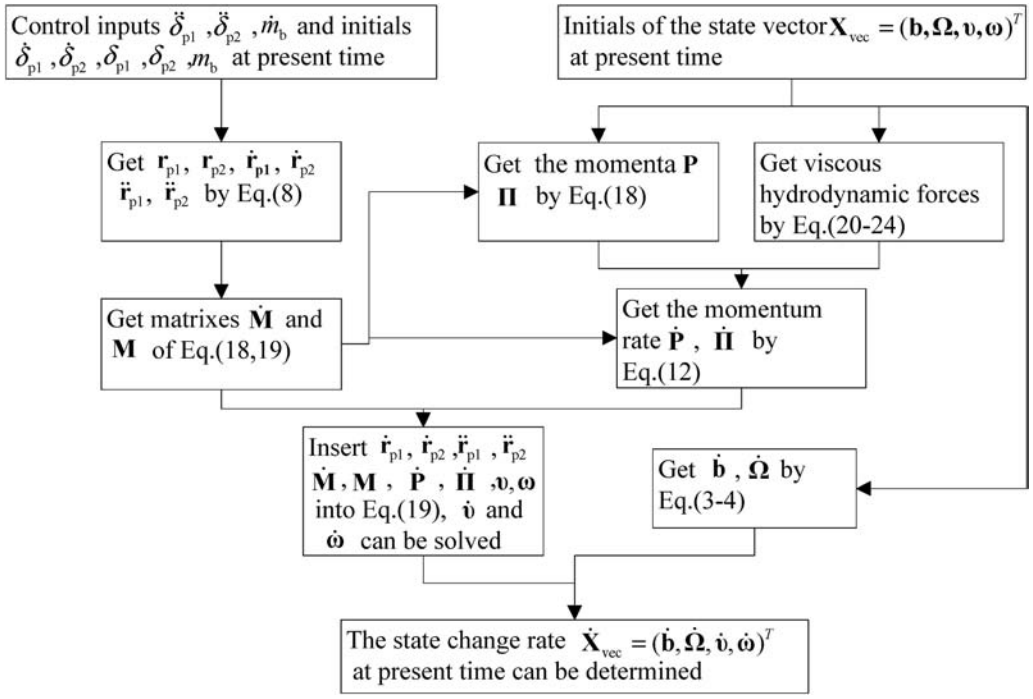

Fig. 7. Flow chart for the calculation of the state change rate.

Table 1
Parameters of the disk type underwater glider.

Parameter	Value
m_{rb}	55.4 kg
$J_{\mathrm{rb}11}$	0.87 kg m^2
$J_{\mathrm{rb}21}$	0 kg m^2
$J_{\mathrm{rb}31}$	0 kg m^2
$r_{\mathrm{rb}1}$	0 m
$r_{\mathrm{b}1}$	0 m
r_0	0.315 m
M_{A11}	0.026 kg
M_{A21}	0 kg
M_{A31}	0 kg
C_{A11}	0 kg m
C_{A21}	0 kg m
C_{A31}	0 kg m
J_{A11}	0.036 kg m^2
J_{A21}	0 kg m^2
J_{A31}	0 kg m^2
X'_{uu}	−0.034
Z'_{w}	−1.68
$K'_{p\|p\|}$	−0.142
$M'_{q\|q\|}$	−0.142
$m_{\mathrm{p}1}$	1 kg
$J_{\mathrm{rb}12}$	0 kg m^2
$J_{\mathrm{rb}22}$	0.87 kg m^2
$J_{\mathrm{rb}32}$	0 kg m^2
$r_{\mathrm{rb}2}$	0 m
$r_{\mathrm{b}2}$	0 m
D	0.9 m
M_{A12}	0 kg
M_{A22}	0.026 kg
M_{A32}	0 kg
C_{A12}	0 kg m
C_{A22}	0 kg m
C_{A32}	0 kg m
J_{A12}	0 kg m^2
J_{A22}	0.036 kg m^2
J_{A32}	0 kg m^2
X'_{ww}	0.453
Z'_{q}	−0.688
M'_{w}	0.31
N'_{r}	-1.2×10^{-3}
$m_{\mathrm{p}2}$	1 kg
$J_{\mathrm{rb}13}$	0 kg m^2
$J_{\mathrm{rb}23}$	0 kg m^2
$J_{\mathrm{rb}33}$	1.61 kg m^2
$r_{\mathrm{rb}3}$	0.0048 m
$r_{\mathrm{b}3}$	0 m
ρ	1000 kg/m^3
M_{A13}	0 kg
M_{A23}	0 kg
M_{A33}	0.838 kg
C_{A13}	0 kg m
C_{A23}	0 kg m
C_{A33}	0 kg m
J_{A13}	0 kg m^2
J_{A23}	0 kg m^2
J_{A33}	5×10^{-5} kg m^2
Y'_{r}	5×10^{-4}
K'_{p}	−0.11
M'_{q}	−0.11
$N'_{r\|r\|}$	-5.14×10^{-4}

the buoyancy in the inertial frame. f_v and τ_v respectively represent viscous hydrodynamic forces and moments in the inertial frame. Note that hydrodynamic forces and moments are constituted of viscous hydrodynamic components and inertial hydrodynamic components. As inertial hydrodynamic components are usually expressed by the added mass, added inertia, and coupling terms which are contained in the kinetic energy of the glider system (Graver, 2005; Wang et al., 2011), only viscous hydrodynamic components are shown in the momentum equations.

Define $\mathbf{P}$ as the expression of $\mathbf{p}$ in the body frame, and $_{\mathbf{\Pi}}$ as the expression of $\boldsymbol{\pi}$ in the body frame, so we can get the transformation equations

$$p = R_{EB}P,\ \boldsymbol{\pi} = R_{EB}\Pi + b \times p \tag{10}$$

Differentiating equations above with respect to time on both sides and utilizing the kinematics expression Eq. (3), we get the following equations

$$\dot{p} = R_{EB}\left(\dot{P} \times \widehat{\omega}P\right),\ \dot{\boldsymbol{\pi}} = R_{EB}\left(\dot{\boldsymbol{\Pi}} + \widehat{\omega}\Pi\right) + R_{EB}v \times p + b \times \dot{\boldsymbol{p}} \tag{11}$$

Substituting Eq. (9) into Eq. (11) will give

$$\begin{aligned}\dot{P} &= P \times \omega + R_{EB}^{T}(G+B) + F_B, \dot{\Pi} \\ &= \Pi \times \omega + P \times v + r_{CG} \times R_{EB}^{T}G + M_B\end{aligned} \tag{12}$$

where r_{CG} is the position vector of the center of gravity in the body frame, $F_B = R_{EB}^{T}f_v$ represents viscous hydrodynamic forces in the body frame, $M_B = R_{EB}^{T}\tau_v$ represents viscous hydrodynamic moments in the body frame.

To derive expressions of P, Π, $\dot{P}$and $\dot{\Pi}$, we need to determine the total kinetic energy of the glider-fluid system. The kinetic energy of the rigid body is

$$T_{rb} = \frac{1}{2}\begin{bmatrix} v \\ \omega \end{bmatrix}^{T}\begin{bmatrix} m_{rb}I & -m_{rb}\widehat{r}_{rb} \\ m_{rb}\widehat{r}_{rb} & J_{rb} \end{bmatrix}\begin{bmatrix} v \\ \omega \end{bmatrix} \tag{13}$$

where I is the3 × 3identity matrix, J_{rb} is the inertia matrix, r_{rb} is the position vector of mass center of m_{rb} in the body frame.

The kinetic energies of the two moving particles are

$$T_{pi} = \frac{1}{2}\begin{bmatrix} v \\ \omega \\ \dot{r}_{pi} \end{bmatrix}^{T}\begin{bmatrix} m_{pi}I & -m_{pi}\widehat{r}_{pi} & m_{pi}I \\ m_{pi}\widehat{r}_{pi} & -m_{pi}\widehat{r}_{pi}\widehat{r}_{pi} & m_{pi}\widehat{r}_{pi} \\ m_{pi}I & -m_{pi}\widehat{r}_{pi} & m_{pi}I \end{bmatrix}\begin{bmatrix} v \\ \omega \\ \dot{r}_{pi} \end{bmatrix} \quad (i = 1,2) \tag{14}$$

where r_{p1} and r_{p2} are position vectors of mass center of blocks p1 and p2 in the body frame.

The kinetic energy of the buoyancy adjustment system is

$$T_b = \frac{1}{2}\begin{bmatrix} v \\ \omega \end{bmatrix}^{T}\begin{bmatrix} m_bI & -m_b\widehat{r}_b \\ m_b\widehat{r}_b & -m_b\widehat{r}_b\widehat{r}_b \end{bmatrix}\begin{bmatrix} v \\ \omega \end{bmatrix} \tag{15}$$

where r_b is the position vector of mass center of m_b in the body frame.

When a glider accelerates in the flow, the surrounding fluid would be affected and also accelerate with the glider. The kinetic energy of the fluid around the glider is

$$T_f = \frac{1}{2}\begin{bmatrix} v \\ \omega \end{bmatrix}^T \begin{bmatrix} M_A & C_A \\ C_A^T & J_A \end{bmatrix} \begin{bmatrix} v \\ \omega \end{bmatrix} \tag{16}$$

where M_A is the added mass matrix, J_A is the added inertia matrix and C_A represents hydrodynamic coupling between the translational and rotational motion of the body.

Finally, we get the total kinetic energy of the glider-fluid system $T = T_{rb} + T_{p1} + T_{p2} + T_f$, and then momenta of the glider and moving mass particles could be calculated by the following equations

$$P = \frac{\partial T}{\partial v},\ \Pi = \frac{\partial T}{\partial \omega},\ P_{p1} = \frac{\partial T}{\partial \dot{r}_{p1}},\ P_{p2} = \frac{\partial T}{\partial \dot{r}_{p2}} \tag{17}$$

where P_{p1} and P_{p2} are momenta of moving mass particles with respect to the body frame.

Then, we can express the momenta in the form of matrix

$$\begin{bmatrix} P \\ \Pi \\ P_{p1} \\ P_{p2} \end{bmatrix} = M \begin{bmatrix} v \\ \omega \\ \dot{r}_{p1} \\ \dot{r}_{p2} \end{bmatrix} \tag{18}$$

where

$$M = \begin{bmatrix} M_A + (m_{rb} + m_{p1} + m_{p2} + m_b)I & C_A - m_{rb}\widehat{r}_{rb} - m_{p1}\widehat{r}_{p1} - m_{p2}\widehat{r}_{p2} - m_b\widehat{r}_b & m_{p1}I & m_{p2}I \\ C_A^T + m_{rb}\widehat{r}_{rb} + m_{p1}\widehat{r}_{p1} + m_{p2}\widehat{r}_{p2} + m_b\widehat{r}_b & J_A + J_{rb} - m_{p1}\widehat{r}_{p1}\widehat{r}_{p1} - m_{p2}\widehat{r}_{p2}\widehat{r}_{p2} - m_b\widehat{r}_b\widehat{r}_b & m_{p1}\widehat{r}_{p1} & m_{p2}\widehat{r}_{p2} \\ m_{p1}I & -m_{p1}\widehat{r}_{p1} & m_{p1}I & 0 \\ m_{p2}I & -m_{p2}\widehat{r}_{p2} & 0 & m_{p2}I \end{bmatrix}$$

Differentiating Eq. (18) with respect to time, then give

$$\begin{bmatrix} \dot{P} \\ \dot{\Pi} \\ \dot{P}_{p1} \\ \dot{P}_{p2} \end{bmatrix} = \dot{M} \begin{bmatrix} v \\ \omega \\ \dot{r}_{p1} \\ \dot{r}_{p2} \end{bmatrix} + M \begin{bmatrix} \dot{v} \\ \dot{\omega} \\ \ddot{r}_{p1} \\ \ddot{r}_{p2} \end{bmatrix} \tag{19}$$

where

$$\dot{M} = \begin{bmatrix} \dot{m}_b I & -m_{p1}\dot{\widehat{r}}_{p1} - m_{p2}\dot{\widehat{r}}_{p2} - \dot{m}_b\widehat{r}_b & 0 & 0 \\ m_{p1}\dot{\widehat{r}}_{p1} + m_{p2}\dot{\widehat{r}}_{p2} + \dot{m}_b\widehat{r}_b & -m_{p1}\dot{\widehat{r}}_{p1}\widehat{r}_{p1} - m_{p1}\widehat{r}_{p1}\dot{\widehat{r}}_{p1} - m_{p2}\dot{\widehat{r}}_{p2}\widehat{r}_{p2} - m_{p2}\widehat{r}_{p2}\dot{\widehat{r}}_{p2} - \dot{m}_b\widehat{r}_b\widehat{r}_b & m_{p1}\dot{\widehat{r}}_{p1} & m_{p2}\dot{\widehat{r}}_{p2} \\ 0 & -m_{p1}\dot{\widehat{r}}_{p1} & 0 & 0 \\ 0 & -m_{p2}\dot{\widehat{r}}_{p2} & 0 & 0 \end{bmatrix}$$

Through Eqs. (18) and (19), it can be seen that P, Π, $\dot{P}$ and $\dot{\Pi}$ could be expressed by combining motion parameters (v, ω, $\dot{v}$,$\dot{\omega}$,$\dot{r}_{p1}$,$\dot{r}_{p2}$, etc) and mass parameters (M_A, C_A, J_A, m_{rb}, m_{p1}, m_{p2}, etc). Then substituting expressions of P, Π, $\dot{P}$and$\dot{\Pi}$ into Eq. (12), the relationship between the motion and forces on the glider in the body frame is established.

2.3. Viscous hydrodynamic forces

Referring to the hydrodynamic analysis of traditional gliders, viscous hydrodynamic forces are usually computed by combining hydrodynamic coefficients and kinematic velocities. This processing method is also adopted in this paper. However, the disk type underwater glider has the omni-maneuverability which is different form conventional underwater vehicles. Viscous hydrodynamic calculation methods of conventional underwater vehicles often became invalid when the velocity component v in the body frame is too large. To address this problem, a new coordinate frame named as "direction coordinate frame" is introduced and the definition of the direction coordinate frame $o - \tilde{x}\tilde{y}\tilde{z}$is shown in Fig. 6. Coordinate axis $o-z$ coincides with that of body frame and coordinate axis $o - \tilde{x}$ points towards the direction of the projection of velocity vector in $o-xy$ plane. The intersection angle between coordinate axis $o - \tilde{x}$ and $o-x$ is defined as β, so we can get

$$cos\beta = u\Big/\sqrt{u^2+v^2},\ sin\beta = v\Big/\sqrt{u^2+v^2} \tag{20}$$

When $u = 0$ and $v = 0$, β is regarded as zero. Then a rotation matrix R_{DB} that maps the vector from the body frame to the direction coordinate frame is defined as

$$R_{DB} = \begin{bmatrix} c\beta & s\beta & 0 \\ -s\beta & c\beta & 0 \\ 0 & 0 & 1 \end{bmatrix} \tag{21}$$

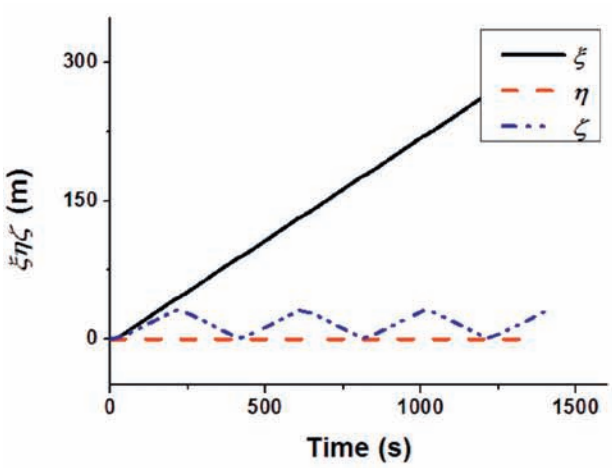

(a) Position of the glider in the inertial system

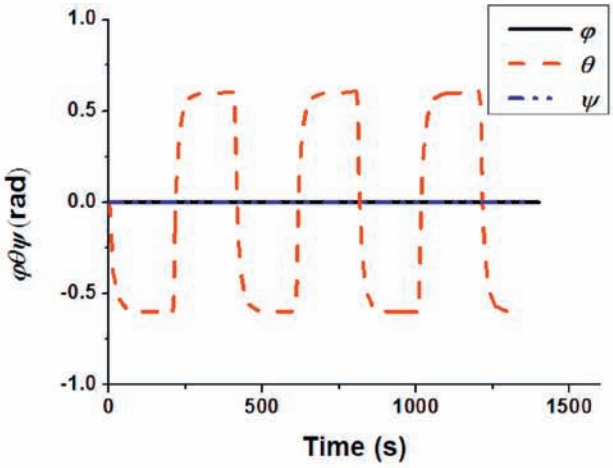

(b) Attitude of the glider in the inertial system

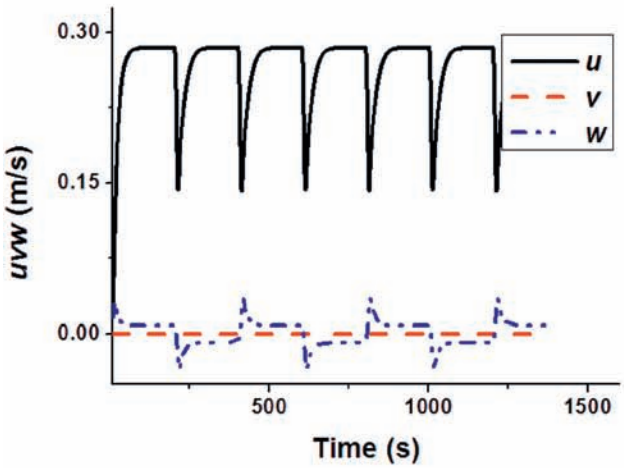

(c) Linear velocity of the glider in the body frame

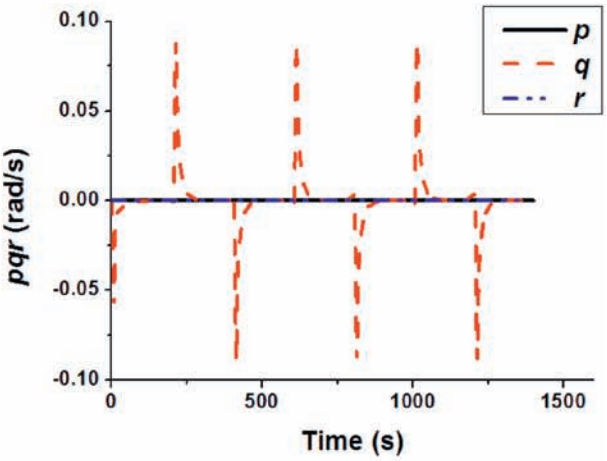

(d) Angular velocity of the glider in the body frame

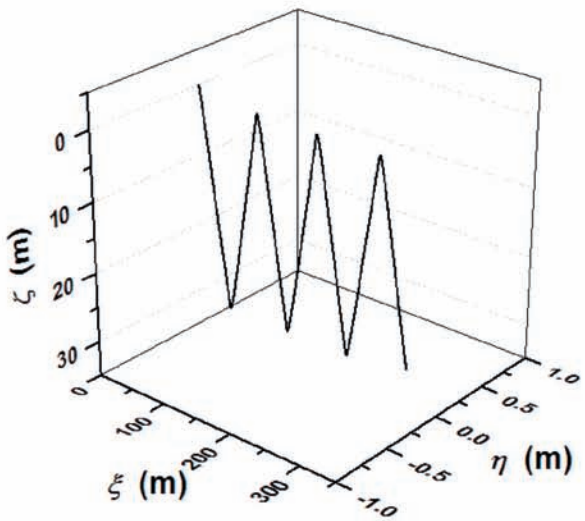

(e) Trajectory in the three-dimensional space

Fig. 8. Behavior of sawtooth motion in horizontal direction.

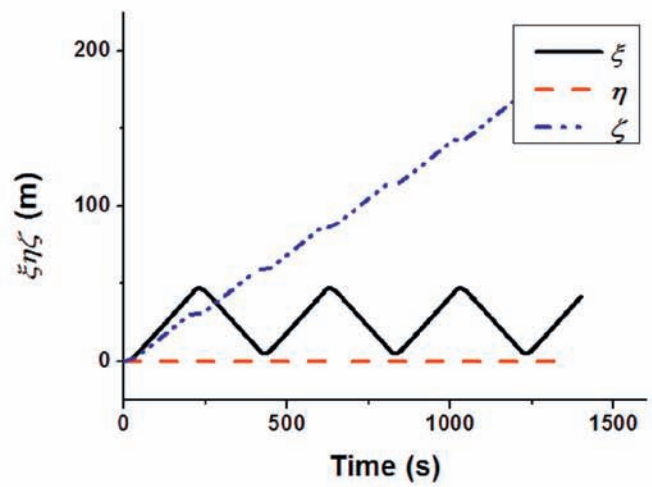

(a) Position of the glider in the inertial system

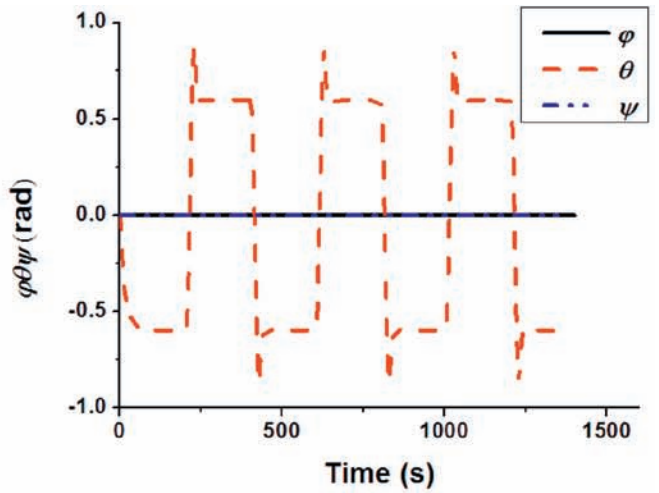

(b) Attitude of the glider in the inertial system

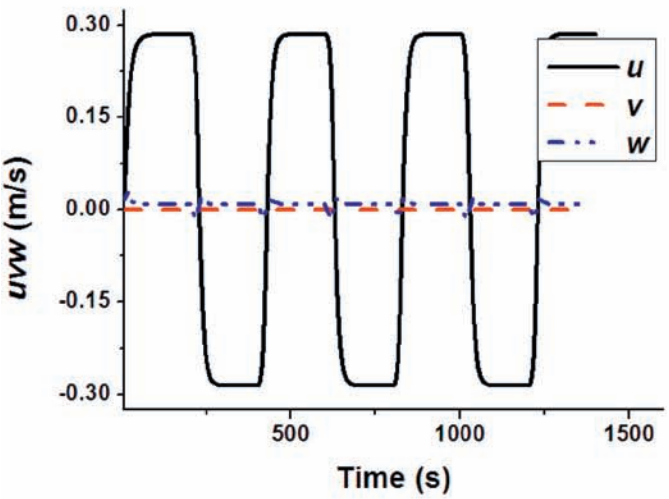

(c) Linear velocity of the glider in the body frame

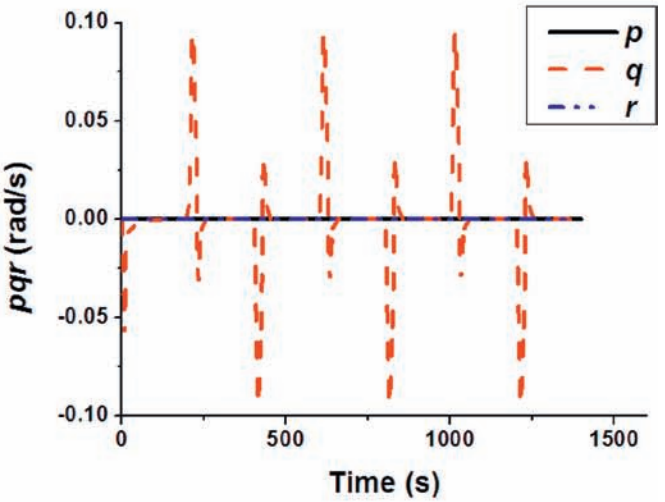

(d) Angular velocity of the glider in the body frame

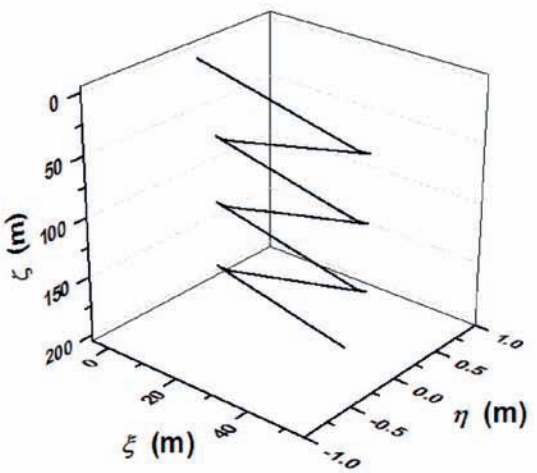

(e) Trajectory in the three-dimensional space

Fig. 9. Behavior of sawtooth motion in vertical direction.

So if $\tilde{v} = (\tilde{u} \quad \tilde{v} \quad \tilde{w})^T$ and $\tilde{\omega} = (\tilde{p} \quad \tilde{q} \quad \tilde{r})^T$ are expressions of the linear and angular velocities with respect to the direction coordinate frame, we can get

$$\tilde{v} = R_{DB}v,\ \tilde{\omega} = R_{DB}\omega \tag{22}$$

Through the transformation above, the velocity component $\tilde{v}$ in the direction coordinate frame would always be zero, which means that the viscous hydrodynamic calculation method of conventional underwater vehicle would be suitable. Then in the direction coordinate frame, the viscous hydrodynamic force $F_D = (F_{DX} \quad F_{DY} \quad F_{DZ})^T$ and hydrodynamic moment $M_D = (M_{DX} \quad M_{DY} \quad M_{DZ})^T$ can be expressed as

$$\begin{aligned}
F_{DX} &= 0.5\rho D^2\left(X'_{uu}\tilde{u}^2 + X'_{ww}\tilde{w}^2\right)\\
F_{DY} &= 0.5\rho D^3 Y'_r\tilde{u}\tilde{r}\\
F_{DZ} &= 0.5\rho D^2 Z'_w\tilde{u}\tilde{w} + 0.5\rho D^3 Z'_q\tilde{u}\tilde{q}\\
M_{DX} &= 0.5\rho D^4 K'_p\tilde{u}\tilde{p} + 0.5\rho D^5 K'_{p|p|}\tilde{p}|\tilde{p}|\\
M_{DY} &= 0.5\rho D^3 M'_w\tilde{u}\tilde{w} + 0.5\rho D^4 M'_q\tilde{u}\tilde{q} + 0.5\rho D^5 M'_{q|q|}\tilde{q}|\tilde{q}|\\
M_{DZ} &= 0.5\rho D^4 N'_r\tilde{u}\tilde{r} + 0.5\rho D^5 N'_{r|r|}\tilde{r}|\tilde{r}|
\end{aligned} \tag{23}$$

where ρ is the fluid density, D is the external diameter of the disk type underwater glider, X'_{uu}, X'_{ww}, Y'_r, Z'_w, Z'_q, K'_p, $K'_{p|p|}$, M'_w, M'_q, $M'_{q|q|}$ and N'_r are non-dimensional hydrodynamic coefficients, which can be calculated computational fluid dynamics or hydrodynamic testing techniques. As the shape of the disk type glider is axisymmetric, non-dimensional hydrodynamic coefficients would not change with β and they can be determined in the body frame.

The rotation matrix R_{DB} also has the property like $R_{DB}^{-1} = R_{DB}^T$, so the viscous hydrodynamic force F_B and hydrodynamic moment M_B in the body frame can be expressed as

$$F_B = R_{DB}^T F_D, M_B = R_{DB}^T M_D \tag{24}$$

2.4. Solution of the dynamic model

Based on the derivation of kinematics, dynamics and hydrodynamics of the disk type underwater glider, the nonlinear dynamic model for three-dimensional motion simulation is established. Obviously, there are lots of variables and equations in the dynamic model of the disk type glider, so it is necessary to analyze the solution process of the dynamic model. As previously introduced, control inputs of the glider system $\dot{\delta}_{p1}$, $\dot{\delta}_{p2}$, $\dot{m}_b$ and initials of control variables δ_{p1}, δ_{p2}, $\dot{\delta}_{p1}$, $\dot{\delta}_{p2}$, m_b are known before simulation. Define $X_{vec} = (b \quad \Omega \quad v \quad \omega)^T$ as the state vector of the glider, so if the state change rate $\dot{X}_{vec} = \left(\dot{b} \quad \dot{\Omega} \quad \dot{v} \quad \dot{\omega}\right)^T$ is calculated with given initials and control inputs, the motion simulation of the glider would be realized by adopting Runge-Kutta fourth-order algorithm. The calculation process of the state change rate is shown in Fig. 7 in general.

3. Motion simulation

In this section, typical motions of a disk type underwater glider (sawtooth motion in horizontal direction, sawtooth motion in vertical direction and omni-directional motion) are simulated based on the nonlinear dynamic model derived above. The parameters of the disk type underwater glider we have designed are listed in Table 1, which includes geometric parameters, physical parameters and hydrodynamic coefficients. As the shape of the glider in this paper is consistent with the disk type underwater glider in Nakamura et al. (2007), the non-dimensional hydrodynamic coefficients of the glider in this paper are referred to the hydrodynamic coefficients in Nakamura et al. (2007), which were determined by model tests.

The environment in the deep sea is similar to the ideal still water environment, and the motion simulation of underwater gliders in the still water is the basis of the motion analysis of underwater gliders in the real ocean environment. Therefore, the motion simulation in the ideal still water environment has attracted many researches (Wang and Wang, 2009; Wang et al., 2011; Fan and Woolsey, 2013). Given initial conditions and the control quantity, the three-dimensional motion of the disk type glider in the still water environment could be realized.

3.1. Sawtooth motion in horizontal direction

The sawtooth motion in horizontal direction is the principal working pattern for conventional gliders. Set the motion initial conditions $\{\xi_B, \eta_B, \zeta_B, \varphi, \theta, \psi, u, v, w, p, q, r\}$ as{0 *m*, 0 *m*, 0 *m*,0 *rad*, 0 *rad*, 0 *rad*, 0 *m/s*, 0 *m/s*, 0 *m/s*, 0 *rad/s*, 0 *rad/s*, 0 *rad/s*}and set the control initial conditions $\{\delta_{p1}, \delta_{p2}, \dot{\delta}_{p1}, \dot{\delta}_{p2}, m_b\}$as {1.57 *rad*, −1.57 *rad*, 0 *rad/s*, 0 *rad/s*, 0 *kg*}. By adjusting the positions of two blocks and the mass of the buoyancy adjustment system in Eqs. (25)−(27), the sawtooth motion in horizontal direction is simulated.

As shown in Fig. 8, the disk type underwater glider also can accomplish the sawtooth motion in horizontal direction like conventional gliders. Under the current control inputs, the pitch angle θ of the glider is about $\pm 34°$, the velocity component u is about 0.285 m/s and the glider advanced about 300 m in horizontal direction during the 1400 s.

$$\dot{m}_b = \begin{cases}
0.008t & 0 < t \le 5\\
0.04 - 0.008(t-5) & 5 < t \le 10\\
0 & 10 < t \le 200\\
(-1)^i \times 0.016 \times (t - 200i) & 200i < t \le 200i + 5,\ i = 1,2,3\ldots\\
(-1)^i \times [0.08 - 0.016 \times (t - 200i - 5)] & 200i + 5 < t \le 200i + 10,\ i = 1,2,3\ldots\\
0 & 200i + 10 < t \le 200i + 200,\ i = 1,2,3\ldots
\end{cases} \tag{25}$$

$$\ddot{\delta}_{p1} = \begin{cases} -0.002t & 0 < t \le 5 \\ -0.01 + 0.002(t-5) & 5 < t \le 15 \\ 0.01 - 0.002(t-15) & 15 < t \le 20 \\ 0 & 20 < t \le 200 \\ (-1)^{i+1} \times 0.004 \times (t - 200i) & 200i < t \le 200i + 5, i = 1,2,3\ldots \\ (-1)^{i+1} \times [0.02 - 0.004 \times (t - 200i - 5)] & 200i + 5 < t < 200i + 15, i = 1,2,3\ldots \\ (-1)^{i+1} \times [-0.02 + 0.004 \times (t - 200i - 15)] & 200i + 15 < t \le 200i + 20, i = 1,2,3\ldots \\ 0 & 200i + 20 < t \le 200i + 200, i = 1,2,3\ldots \end{cases} \tag{26}$$

$$\ddot{\delta}_{p2} = -\ddot{\delta}_{p1} \tag{27}$$

3.2. Sawtooth motion in vertical direction

The sawtooth motion in vertical direction is a special motion pattern for the disk type underwater gliders. Set the motion initial conditions $\{\xi_B, \eta_B, \zeta_B, \varphi, \theta, \psi, u, v, w, p, q, r\}$ as{0 *m*, 0 *m*, 0 *m*, 0 *rad*, 0 *rad*, 0 *rad*, 0 *m/s*, 0 *m/s*, 0 *m/s*, 0 *rad/s*, 0 *rad/s*, 0 *rad/s*} and set the control initial conditions $\{\delta_{p1}, \delta_{p2}, \dot{\delta}_{p1}, \dot{\delta}_{p2}, m_b\}$as {1.57 *rad*, −1.57 *rad*, 0 *rad/s*, 0 *rad/s*, 0 *kg*}. By adjusting the positions of two blocks as Eqs. (26) and (27) and adjusting the mass of the buoyancy adjustment system as Eq. (28), the sawtooth motion in vertical direction is simulated.

$$\dot{m}_b == \begin{cases} 0.008t & 0 < t \le 5 \\ 0.04 - 0.008(t-5) & 5 < t \le 10 \\ 0 & 10 < t \end{cases} \tag{28}$$

As shown in Fig. 9, the sawtooth motion in vertical direction would realize the detection of a fixed water area at different depth. Under the current control inputs, the pitch angle θ of the glider is about $\pm 34^\circ$, the velocity component u is about ± 0.285 m/s and the glider advanced about 200 m in vertical direction during the 1400s.

3.3. Omni-directional motion for virtual mooring

As the disturbance of ocean currents, the position of the glider may beyond the region of virtual mooring and the glider should return to its mooring region during its next gliding. For conventional gilders, they usually adopt turning actions to change the gliding direction which usually required a large space and a long time. However, the disk type underwater glider could change the gliding direction without rotation of the glider and this motion characteristic makes them suitable for virtual mooring. Set the motion initial conditions $\{\xi_B, \eta_B, \zeta_B, \varphi, \theta, \psi, u, v, w, p, q, r\}$ as{0 *m*, 0 *m*, 0 *m*, 0 *rad*, 0 *rad*, 0 *rad*, 0 *m/s*, 0 *m/s*, 0 *m/s*, 0 *rad/s*, 0 *rad/s*, 0 *rad/s*} and the control initial conditions $\{\delta_{p1}, \delta_{p2}, \dot{\delta}_{p1}, \dot{\delta}_{p2}, m_b\}$ of different gliding lines are shown in Table 2. By adjusting the buoyancy adjustment system as Eq. (28), omni-directional motion for virtual mooring is simulated. As shown in Fig. 10, under different control inputs, the disk type glider can glide in different directions without the rotation of the body. Taking Line 1 as an example, the linear velocity and angular velocity become steady at about 60s as shown in Fig. 11.

The motion simulation of given initial conditions in Table 2 is used to demonstrate the ability of a disk type underwater glider to glide in any direction around the body. In practical applications, positions of two movable blocks should be determined by the movement direction and the incline angle of the glider, as shown in Fig. 3.

Table 2
Control initial conditions.

	δ_{p1} (rad)	δ_{p2} (rad)	$\dot{\delta}_{p1}$ (rad/s)	$\dot{\delta}_{p2}$ (rad/s)	m_b (kg)
Line 1	0.18	4.02	0	0	0.20
Line 2	2.26	6.10	0	0	0.20
Line 3	3.32	0.87	0	0	0.20
Line 4	5.41	2.96	0	0	0.20

4. Conclusions

This paper concentrates on nonlinear dynamics modeling and motion simulation of the disk type underwater glider. Through the analysis of kinematics, dynamics and hydrodynamics of the disk type underwater glider, a reasonable

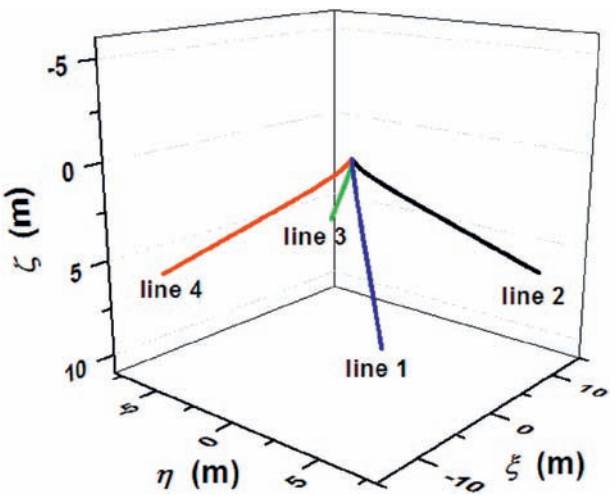

Fig. 10. Trajectories in the three-dimensional space.

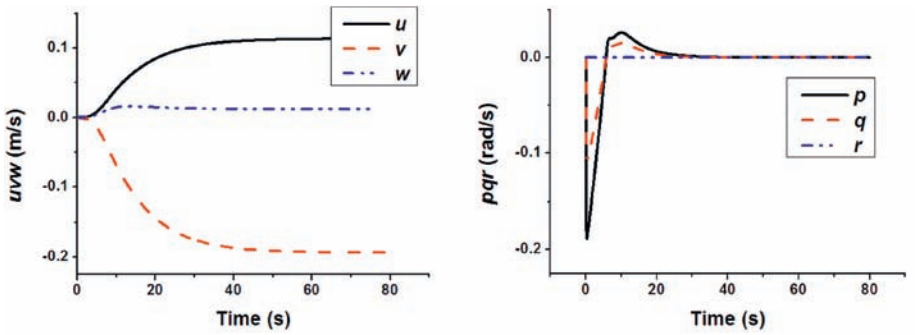

(a) Linear velocity of the glider in the body frame (b) Angular velocity of the glider in the body frame

Fig. 11. Velocity variation of Line 1.

dynamic model that considers the effect of internal masses movement and the omni-maneuverability is derived. Based on the dynamic model, typical motions of the disk type underwater glider are simulated and it is find that the disk type underwater glider can not only complete the horizontal sawtooth motion of conventional underwater gliders, but also perform some special actions, such as sawtooth motion in vertical direction and omni-directional motion for virtual mooring. The simulation results show that the dynamic model is feasible and the disk type glider has good maneuverability.

The prototype of a disk type underwater glider would be developed in the future. And experiments of the glider in the laboratory (Zhang et al., 2014) and the field (Wang et al., 2011; Zhang et al., 2016; Jiao et al., 2016) would be carried out. Through comparing the theoretical and experimental values of the motion response, the theoretical method in this paper would be further validated.

Acknowledgments

This work is supported by the National Key Research and Development Program of China (Nos. 2016YFC0301500) and the Fundamental Research Funds for the Central Universities (3132017032).

References

Bhatta, P., Leonard, N.E., 2008. Nonlinear gliding stability and control for vehicles with hydrodynamic forcing. Automatica 44 (5), 1240–1250.

Chen, Z., Yu, J., Zhang, A., Zhang, F., 2016. Design and analysis of folding propulsion mechanism for hybrid-driven underwater gliders. Ocean. Eng. 119, 125–134.

Eriksen, C.C., Osse, T.J., Light, R.D., Wen, T., Lehman, T.W., Sabin, P.L., Ballard, J.W., Chiodi, A.M., 2001. Seaglider: a long-range autonomous underwater vehicle for oceanographic research. IEEE J. Ocean. Eng. 26 (4), 424–436.

Fan, S., Woolsey, C., 2013. Elements of underwater glider performance and stability. Mar. Technol. Soc. J. 47 (3), 81–98.

Graver, J.G., 2005. Underwater Gliders: Dynamics, Control and Design. Doctor, Princeton University.

Isa, K., Arshad, M.R., Ishak, S., 2014. A hybrid-driven underwater glider model, hydrodynamics estimation, and an analysis of the motion control. Ocean. Eng. 81, 111–129.

Jiao, J., Ren, H., Sun, S., Liu, N., Li, H., Adenya, C.A., 2016. A state-of-the-art large scale model testing technique for ship hydrodynamics at sea. Ocean. Eng. 123, 174–190.

Leonard, N.E., Graver, J.G., 2001. Model-based feedback control of autonomous underwater gliders. IEEE J. Ocean. Eng. 26 (4), 633–645.

Mahmoudian, N., Geisbert, J., Woolsey, C., 2010. Approximate analytical turning conditions for underwater gliders: implications for motion control and path planning. IEEE J. Ocean. Eng. 35 (1), 131–143.

Nakamura, M., Hyodo, T., Koterayama, W., 2007. "LUNA" Testbed vehicle for virtual mooring. In: 17th 2007 International Offshore and Polar Engineering Conference, ISOPE 2007, July 1, 2007–July 6, 2007. International Society of Offshore and Polar Engineers, Lisbon, Portugal.

Nakamura, M., Koterayama, W., Inada, M., Marubayashi, K., Hyodo, T., Yoshimura, H., Morii, Y., 2008. Disk-type underwater glider for virtual mooring and field experiment. In: 18th 2008 International Offshore and Polar Engineering Conference, ISOPE 2008, July 6, 2008–July 11, 2008. International Society of Offshore and Polar Engineers, Vancouver, BC, Canada.

Niewiadomska, K., Jones, C.P., Webb, D.C., 2003. Design of a mobile and bottom resting autonomous underwater gliding vehicle. In: Proceedings of the 13th International Symposium on Unmanned Untethered Submersible Technology, Durham New Hampshire, America.

Sherman, J., Davis, R.E., Owens, W.B., Valdes, J., 2001. The autonomous underwater glider "Spray". IEEE J. Ocean. Eng. 26 (4), 437–446.

Wang, S., Sun, X., Wang, Y., Wu, J., Wang, X., 2011. Dynamic modeling and motion simulation for a winged hybrid-driven underwater glider. China Ocean. Eng. 25 (1), 97–112.

Wang, Y., Wang, S., 2009. Dynamic modeling and three-dimensional motion analysis of underwater gliders. China Ocean. Eng. 23 (3), 489–504.

Webb, D.C., Simonetti, P.J., Jones, C.P., 2001. SLOCUM: an underwater glider propelled by environmental energy. IEEE J. Ocean. Eng. 26 (4), 447–452.

Zhang, F., Ennasr, O., Litchman, E., Tan, X., 2016. Autonomous sampling of water columns using gliding robotic fish: algorithms and harmful-algae-sampling experiments. IEEE Syst. J. 10 (3), 1271–1281.

Zhang, F., Thon, J., Thon, C., Tan, X., 2014. Miniature underwater glider: design and experimental results. IEEE/ASME Trans. Mechatronics 19 (1), 394–399.

Zhang, F., Zhang, F., Tan, X., 2012. Steady spiraling motion of gliding robotic fish. In: 25th IEEE/RSJ International Conference on Robotics and Intelligent Systems, IROS 2012, October 7, 2012–October 12, 2012. Institute of Electrical and Electronics Engineers Inc, Vilamoura, Algarve, Portugal.

Zhang, S., Yu, J., Zhang, A., Zhang, F., 2011. Steady three dimensional gliding motion of an underwater glider. In: 2011 IEEE International Conference on Robotics and Automation, ICRA 2011, May 9, 2011–May 13, 2011. Institute of Electrical and Electronics Engineers Inc, Shanghai, China.

Zhang, S., Yu, J., Zhang, A., Zhang, F., 2013. Spiraling motion of underwater gliders: modeling, analysis, and experimental results. Ocean. Eng. 60, 1–13.